Myocardial Hemodynamics, Physiology, and Perfusion With an Axial Flow Left Ventricular Assist Device in the Calf

Egemen Tuzun, Kazuhiro Eya, Hyun Keun Chee, Jeff L. Conger, Natalie K. Bruno, O. H. Frazier, and Kamuran A. Kadipasaoglu

The Jarvik 2000 axial flow left ventricular assist device (LVAD) is used clinically as a bridge to transplantation or as destination therapy in end-stage heart disease. The effect of the pump's continuous flow output on myocardial and end-organ blood flow has not been studied experimentally. To address this, the Jarvik 2000 pump was implanted in eight calves and then operated at speeds ranging from 8,000 to 12,000 rpm. Micromanometry, echocardiography, and blood oxygenation measurements were used to assess changes in hemodynamics, cardiac dimensions, and myocardial metabolism, respectively, at different speeds as compared with baseline (pump off, 0 rpm) in this experimental model. Microsphere studies were performed to assess the effects on heart, kidney, and brain perfusion at different speeds. The Jarvik 2000 pump unloaded the left ventricle and reduced end-diastolic pressures and left ventricular dimensions, particularly at higher pump speeds. The ratio of myocardial oxygen consumption to coronary blood flow and the ratio of subendocardial to subepicardial blood flow remained constant. Optimal adjustment of pump speed and volume status allowed opening of the aortic valve and contribution of the native left ventricle to cardiac output, even at the maximum pump speed. Neither brain nor kidney microcirculation was adversely affected at any pump speed. We conclude that the Jarvik 2000 pump adequately unloads the left ventricle without compromising myocardial metabolism or end-organ perfusion. *ASAIO Journal* 2004; 50:47–53.

The Jarvik 2000 left ventricular assist device (LVAD) (Jarvik Heart, Inc., New York, NY) is a small, intraventricular, easily implantable axial flow pump designed to be used either for bridging to transplantation or for permanent mechanical circulatory support in end-stage heart disease.[1] It is suitable for use in smaller adults and children.[2] The advantage of the intraventricular position is the elimination of problems related to inlet graft kinking, stagnation, and thrombosis. Additionally, the Jarvik 2000 pump prevents suction of the septal or left ventricular (LV) free walls, does not cause significant hemolysis, and is associated with a low risk of infection.[3]

However, it is not known how the continuous flow output of the Jarvik 2000 pump may affect blood flow to the myocardium or other end organs, such as the liver, kidney, and brain. In their experimental study, Saito *et al.*[4] found that long term continuous blood flow was well tolerated by healthy sheep and produced no functional or histologic changes in the myocardium, brain, kidney, or liver. In a study by Merhige *et al.*,[5] changes in regional myocardial perfusion were measured with microspheres in the presence and absence of ischemia in dogs supported by a continuous flow pump, and the pump was found to increase blood flow in the ischemic myocardial region. On the other hand, Sezai *et al.*[6] found that, as compared with continuous circulation, pulsatile circulation provided more blood to satisfy the physiologic demands of the major organs (myocardium, kidney, and liver) and better microcirculation at the cellular level in ischemic pigs. In this context of contradictory reports, we assessed the relationships between continuous pump flow and changes in LV mechanics and end-organ perfusion in an acute, nonischemic calf model.

Materials and Methods

Jarvik 2000 Axial Flow Pump

The Jarvik 2000 LVAD is a compact, axial-flow impeller pump that consists of a blood pump, a percutaneous power cable, a pump speed controller, and an external direct current power supply. The pump's design has been described in detail elsewhere.[7]

Animal Model

Eight Corriente crossbred calves weighing 92 to 130 kg were used in the study. All calves received humane care in compliance with the *Principles of Laboratory Animal Care* (National Society of Medical Research) and the *Guide for the Care and Use of Laboratory Animals* (National Institutes of Health publication no. 85-23, revised 1996). Our Institutional Animal Care and Use Committee approved all protocols used in the present study.

Anesthesia and Surgical Preparation

A standard anesthesia protocol was followed. Food was withheld from each calf 12 hours before induction of anesthesia. Each calf was premedicated with glycopyrrolate (0.02 mg/kg) intramuscularly (IM) and xylazine (0.2–0.7 mg/kg) IM. A 12 Fr triple lumen venous catheter was inserted percutaneously into the right external jugular vein. Anesthesia was induced with intravenous ketamine (10–20 mg/kg). A cuffed endotracheal tube and an orogastric decompression tube were

From the Cardiovascular Research Laboratories, Texas Heart Institute at St. Luke's Episcopal Hospital, Houston, Texas.

Submitted for consideration June 2003; accepted for publication in revised form October 2003.

Reprint requests: Dr. Kamuran A. Kadipasaoglu, Texas Heart Institute, P.O. Box 20345, MC 3-147, Houston, TX 77225-0345; E-mail kamurank@heart.thi.tmc.edu.

DOI: 10.1097/01.MAT.0000104819.23235.2F

Copyright © American Society of Artificial Internal Organs. Unauthorized reproduction of this article is prohibited.

inserted. General anesthesia was maintained with isoflurane (1.0–3.0%) in oxygen (40–100%). The anesthetized calf was then placed on the operating table in the right lateral decubitus position in preparation for a left thoracotomy and left neck cutdown. Electrocardiographic leads were connected, and a rectal temperature probe was inserted.

Implantation Operation

The Jarvik 2000 pump was implanted through a left thoracotomy during partial cardiopulmonary bypass (CPB). The left carotid artery and jugular vein were exposed for CPB cannulation. A left thoracotomy was then performed in the fourth intercostal space. The fifth rib was removed to expose the apex of the left ventricle and the descending thoracic aorta. The pericardium was incised from the apex to the pulmonary artery, and the heart was suspended in a pericardial cradle. Heparin (3 mg/kg) was administered. Then, a 22 Fr cannula was placed in the left common carotid artery, and a 28 Fr wire reinforced venous cannula was advanced through the left external jugular vein to the right atrium. The calf's body temperature was cooled to between 30°C and 32°C, and all cannulae were connected to the CPB circuit (Terumo SX-10 membrane oxygenator and Terumo roller pump; Terumo, Inc., Tokyo, Japan).

Next, the 16 mm Dacron outflow graft of the Jarvik 2000 pump was anastomosed to the descending thoracic aorta with a 4–0 propylene suture while aortic flow was temporarily impeded with a partially occluding vascular clamp. CPB was initiated, and the heart was fibrillated. A silicone/polyester sewing cuff was sewn to the ventricular apex with pledgeted, coated, braided 2–0 polyester mattress sutures. The Jarvik 2000 pump was then inserted into the ventricular apex and secured with cotton tape around the cuff and pump casing. After the pump was secured, air was removed from the left ventricle, pump, and graft. Once the calf's body temperature was normalized (37.7–38.8°C), the heart was defibrillated and paced if necessary. The calf was then slowly weaned from CPB.

Intraoperative Hemodynamic Assessment

Once surgery was completed, the venous cannula was removed, and an 8 Fr Swan-Ganz catheter was inserted into the pulmonary artery *via* the left external jugular vein. The carotid arterial cannula was removed to insert a special catheter fitted with a high fidelity micromanometer tip (Millar Mikro-Tip Catheter, Millar Instruments, Houston, TX) into the left ventricle. A pressure catheter was inserted *via* the left internal thoracic artery and advanced proximally into the immediate vicinity of the aortic valve to measure arterial pressure. Four different ultrasonic flow probes (Transonics Inc., Ithaca, NY) were then placed as follows (**Figure 1**): a 16 mm flow probe on the outflow graft, a 24 mm probe 2 cm cranial from the site of anastomosis on the descending thoracic aorta, a 16 mm probe on the brachiocephalic artery 2 cm above its bifurcation from the aorta, and a 3 mm probe around the proximal left anterior descending coronary artery. Data were recorded by a 16 channel computer data acquisition system (Ponemah System version 3.3, Gould Instrument Systems Inc., Valley View, OH).

Hemodynamics were assessed for 20 minutes at each of several pump settings in sequence: first with the pump off and the outflow graft clamped to avoid pump regurgitation (0 rpm) (baseline) and then stepwise with the pump operating at various increasing speeds (8,000, 9,000, 10,000, 11,000, and 12,000 rpm). At each speed, the pump was allowed to operate for 10 minutes to allow cardiac recovery before hemodynamic data collection began. The data that were gathered included mean heart rate (HR), systolic pressure (AoP_s), diastolic pressure (AoP_d), mean aortic pressure (AoP_m), mean pulmonary artery pressure (PAP), pulmonary capillary wedge pressure (PCWP), central venous pressure (CVP), LV systolic pressure (LVP), LV end-diastolic pressure (LVEDP), and flow rates.

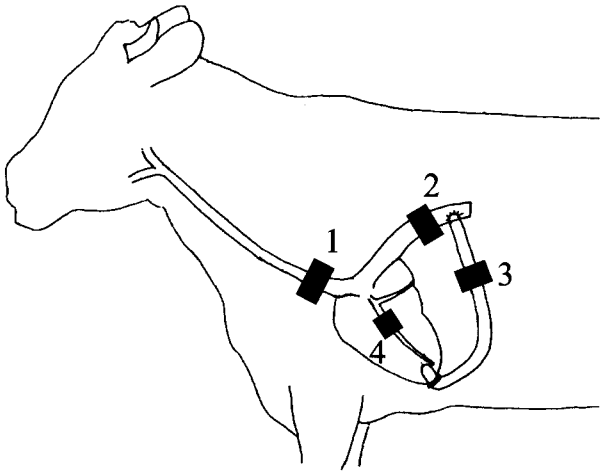


Figure 1. Schematic of instrumentation technique. Black bars show the placement of ultrasonic flow probes on the brachiocephalic artery (1), descending thoracic aorta (2), pump outflow graft (3), and proximal left anterior descending coronary artery (4).

Echocardiographic Assessment

Serial two-dimensional transepicardial studies were performed at baseline and at each pump speed. Echocardiographic assessment was accomplished using a Hewlett Packard Sonos 2000 ultrasound system equipped with a 2.5 MHz phased array transducer, according to the guidelines of the American Society of Echocardiography.[8] The echocardiogram was used to measure systolic and diastolic LV internal dimensions (LVISd and LVIDd), aortic valve motion, and LV wall motion.

Myocardial Oxygen Consumption Assessment

An 18 gauge angiocatheter was inserted into the coronary sinus *via* the azygos vein to take coronary sinus blood samples. One blood sample was taken at baseline and at each pump speed to assess myocardial oxygen consumption (MVO_2). MVO_2 was approximated as the difference between aortic ($\bar{a}$) and coronary sinus ($\bar{v}$) blood oxygen content, multiplied by the left anterior descending (LAD) coronary artery blood flow rate (CBF) (*i.e.*, $MVO_2 = CBF \cdot \bar{a} - \bar{v}$). A Novastat Profile M blood gas analyzer (Nova Biomedical Co., Waltham, MA) was used for blood gas analysis.

Copyright © American Society of Artificial Internal Organs. Unauthorized reproduction of this article is prohibited.

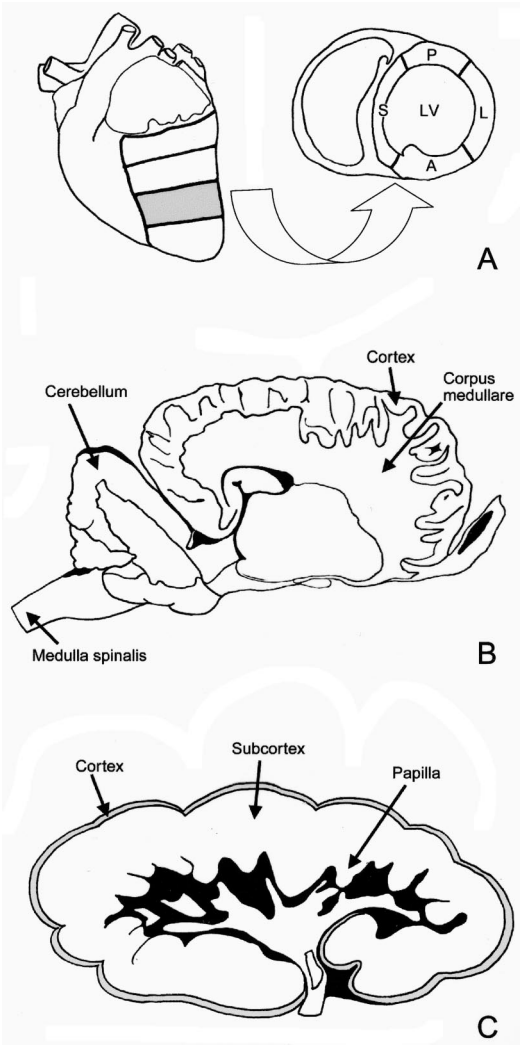


Figure 2. Schematics of tissue sections used in assessing perfusion in the heart (A), brain (B), and kidney (C). S, septal wall; A, anterior wall; L, lateral wall; LV, left ventricle; P, posterior wall.

Tissue Perfusion Assessment

Tissue perfusion was assessed by microsphere analysis using 15 μm, nonradioactive, stable isotope–labeled microspheres (BioPAL, Inc., Worcester, MA). The microspheres were injected, according to the manufacturer's suggested standards, into the left atrium while the pump was off or operating at 8,000, 9,000, 10,000, 11,000, and 12,000 rpm. Microspheres labeled with gold appeared red, those labeled with lanthanum appeared blue, those labeled with antimony appeared violet, and those labeled with lutetium appeared pink. Each labeled microsphere was used at a different pump speed.

After tissue perfusion assessment, each calf was euthanized. Then, its heart, brain, and left kidney were harvested for analysis as follows. In the case of the heart, the left ventricle was isolated and divided into four equal transverse sections along the atrioventricular groove (**Figure 2A**). The basal and apical sections were discarded. The more distal of the remaining two sections was selected and divided into four segments representative of the septal, anterior, lateral, and posterior walls (**Figure 2A**). Each segment was further divided into an epicardial and an endocardial subregion. Two grams of tissue were taken from each region (a total of eight cardiac tissue samples) for microsphere analysis.

The left hemisphere of the brain, the cerebellum, and the upper 3 cm of the medulla spinalis were each divided into three equal parts posteroanteriorly, and the middle sections were harvested. Two grams of tissue were taken from each of the cortex, corpus medullare, cerebellum, and medulla spinalis subregions (a total of four brain tissue samples) for microsphere analysis (**Figure 2B**).

The left kidney was divided into three frontal sections, and the middle section was divided into cortical, subcortical, and papillary subregions. Two grams of tissue were taken from each subregion (a total of three kidney tissue samples) for microsphere analysis (**Figure 2C**).

All tissue samples were dried overnight at 70°C and sent out for analysis. Blood samples were obtained and used to normalize tissue sample readings. The analysis was based upon an

Table 1. Left and Right Heart Hemodynamic Measurements

	Pump Speed (rpm)					
	Pump Off (Baseline)	8,000	9,000	10,000	11,000	12,000
HR (bpm)	78 ± 14	80 ± 14	77 ± 16	77 ± 17	78 ± 15	78 ± 14
Aortic pressure (mm Hg)						
Systolic	80 ± 9	83 ± 7	84 ± 9	84 ± 9	85 ± 9	85 ± 9
Diastolic	61 ± 12	65 ± 8	70 ± 10	72 ± 9	74 ± 12	74 ± 13
Mean	71 ± 9	74 ± 8	76 ± 10	77 ± 9	77 ± 11	77 ± 13
LVP (mm Hg)	84 ± 12	83 ± 8	83 ± 8	77 ± 15	54 ± 21**	42 ± 22***
LVEDP (mm Hg)	11 ± 3	10 ± 3	9 ± 3	9 ± 4	7 ± 3*	6 ± 5*
Maximal dP/dt	1488 ± 638	1470 ± 673	1372 ± 693	1213 ± 780	862 ± 608	749 ± 559*
PCWP (mm Hg)	12 ± 2	11 ± 4	11 ± 4	10 ± 4	9 ± 4	8 ± 5
CVP (mm Hg)	12 ± 6	12 ± 6	13 ± 6	13 ± 6	13 ± 6	13 ± 5
CO (L/min)	7.1 ± 0.9	6.7 ± 1	6.3 ± 1.1	6.3 ± 1.2	6.3 ± 2	6.7 ± 1.6

Values are mean ± SD. bpm, beats per minute; CO, cardiac output; CVP, central venous pressure; dP/dt, rate of change of LVP over time; HR, heart rate; LVEDP, left ventricular end-diastolic pressure; LVP, left ventricular systolic pressure; PCWP, pulmonary capillary wedge pressure.

* $p < 0.05$ *vs.* baseline.

** $p < 0.01$ *vs.* baseline.

*** $p < 0.001$ *vs.* baseline.

Copyright © American Society of Artificial Internal Organs. Unauthorized reproduction of this article is prohibited.

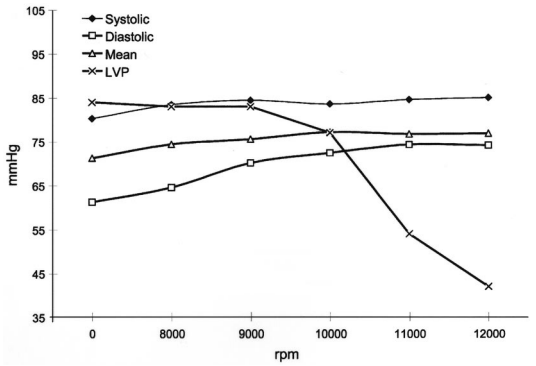


Figure 3. Peak aortic blood pressures and peak left ventricular pressure (LVP).

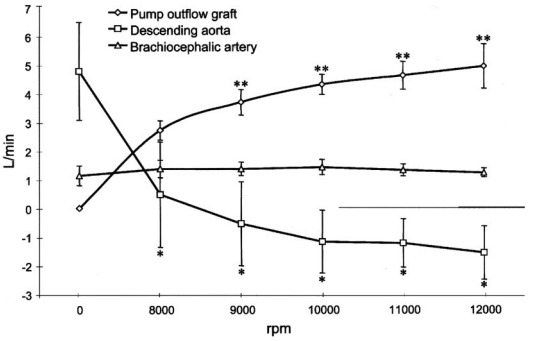


Figure 5. Blood flow in descending aorta, brachiocephalic artery, and pump outflow graft. *$p < 0.001$ *vs.* baseline; **$p < 0.05$ *vs.* 8,000 rpm.

automated neutron activation system described in detail elsewhere.[9–11]

Statistical Analysis

All statistical tests were performed using Microsoft Excel or SAS (SAS Institute, Inc., Cary, NC) software on a personal computer. A value of $p < 0.05$ was considered significant. The power was 80%. Student's t-test was used whenever two continuous variables were compared.

Results

All experiments were successfully completed without surgical or mechanical (device) complications. After rewarming, the mean body temperature of the animals throughout the data collection phase was 38.2 ± 6°C.

Hemodynamic Studies

Table 1 shows the data obtained from left and right heart catheterization. As pump speed increased above 10,000 rpm, mean AoP_d increased progressively but not significantly ($p = 0.07$ for 10,000, 11,000, and 12,000 rpm *vs.* baseline). The increases in mean AoP_s and AoP_m were less pronounced, and as a result, the aortic pulse pressure narrowed from 21 ± 8 mm Hg at baseline to 11 ± 6 mm Hg at 12,000 rpm ($p = 0.08$ *vs.* baseline) (**Figure 3**). Mean CVP and PAP were not affected by variations in pump speed.

Mean LVP did not change significantly between 8,000 and 10,000 rpm but fell sharply at 11,000 rpm ($p < 0.01$ *vs.* baseline). Depending upon the extent of LV unloading, mean LVEDP and PCWP also decreased at speeds of 11,000 and 12,000 rpm ($p < 0.05$ for LVEDP and $p = 0.07$ for PCWP *vs.* baseline) (**Figure 4**). The systolic pressure gradient between the left ventricle and the aorta (LVP – AoP) was 4 mm Hg at baseline and decreased to −31 mm Hg at 11,000 rpm and −43 mm Hg at 12,000 rpm, in favor of systemic pressures.

All baseline blood flow data were collected when the pump was off and the outflow graft clamped. After the pump was activated and the clamp released, the mean pump flow gradually rose from 2.72 ± 0.33 L/min (34% ± 0.2% of cardiac output) at 8,000 rpm to 4.94 ± 0.77 L/min (73% ± 2% of cardiac output) at 12,000 rpm ($p < 0.001$ for all speeds *vs.* 8,000 rpm) (**Figure 5**). On the other hand, the mean blood flow in the descending aorta dropped from 4.84 ± 1.7 L/min at baseline to 0.47 ± 1.83 L/min as soon as the pump began operating at 8,000 rpm. At 8,500 rpm, the blood flow reversed direction and began flowing from the graft anastomosis towards the aortic root at a rate of 0.55 ± 1.46 L/min. At higher pump speeds, this reversed flow gradually increased until it reached 1.56 ± 0.93 L/min at 12,000 rpm ($p < 0.001$ for all speeds *vs.* baseline). The mean brachiocephalic arterial blood flow did not vary with increasing pump speed.

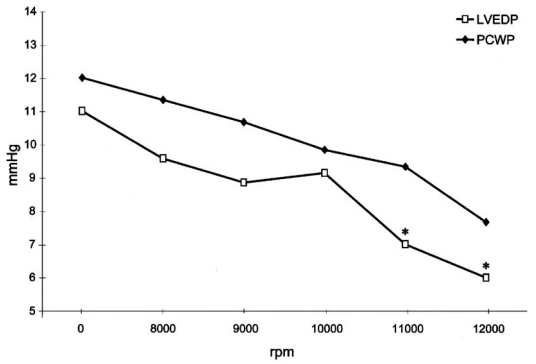


Figure 4. Left ventricular end-diastolic pressure (LVEDP) and pulmonary capillary wedge pressure (PCWP). *$p < 0.001$ *vs.* baseline.

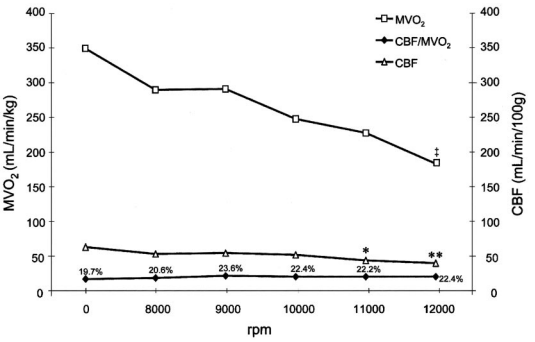


Figure 6. Coronary blood flow (CBF), myocardial oxygen consumption (MVO_2), and CBF/MVO_2 ratio. *$p < 0.05$ *vs.* baseline; **$p < 0.01$ *vs.* baseline; ‡$p < 0.001$ *vs.* baseline.

Copyright © American Society of Artificial Internal Organs. Unauthorized reproduction of this article is prohibited.

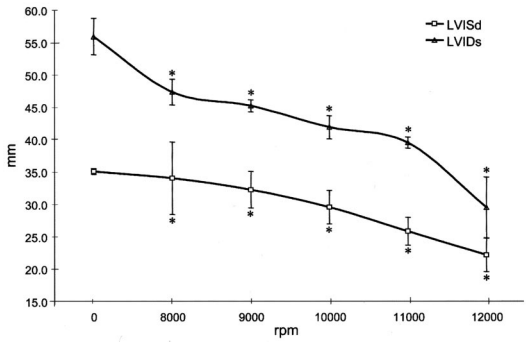


Figure 7. Left ventricular internal systolic dimension (LVISd) and left ventricular internal diastolic dimension (LVIDd). *$p < 0.001$ *vs.* baseline.

Mean CBF decreased slightly between 8,000 and 10,000 rpm but then dropped significantly between 11,000 and 12,000 rpm ($p < 0.05$ and $p < 0.01$ *vs.* baseline, respectively) (**Figure 6**). The fall in mean MVO_2 levels was consistent with and steeper than the fall in CBF, nearing statistical significance at 10,000 and 11,000 rpm ($p = 0.08$ and $p = 0.07$, respectively) and becoming highly significant at 12,000 rpm ($p < 0.001$). Despite the decreasing CBF and MVO_2 levels at increasingly higher pump speeds, the baseline ratio of CBF to MVO_2 was well preserved at all speeds and remained between 0.19 and 0.22 throughout the study.

Echocardiographic Studies

Epicardial echocardiography confirmed the unloading effect of the Jarvik 2000 pump at increasingly higher speeds. At 12,000 rpm, mean LVISd decreased from a baseline value of 35.1 ± 0.4 mm to 22.1 ± 2.6 mm, whereas mean LVIDd decreased from a baseline value of 55.9 ± 2.8 mm to 29.5 ± 4.7 mm. Systolic and diastolic LV dimensions were significantly below baseline levels at all speeds ($p < 0.001$) (**Figure 7**). Aortic valve opening was impaired in one calf at 10,000 rpm, in two calves at 11,000 rpm, and in four calves at 12,000 rpm. Septal and lateral wall motion was not affected by increasing pump speed, and right heart pressures remained close to baseline levels.

Tissue Perfusion

At increasing pump speeds, blood flow in myocardial subregions (*i.e.*, subendocardium and subepicardium) gradually decreased below baseline levels in all segments (septal, lateral, anterior, and posterior) (**Table 2**). Endocardial blood flow in the LV free wall, which was calculated as the sum of the anterior, lateral, and posterior endocardial blood flows, was significantly reduced below baseline at 10,000 and 12,000 rpm ($p < 0.05$ and $p < 0.01$, respectively). Similarly, epicardial blood flow in the LV free wall decreased at increasing pump speeds to levels that approached statistical significance at 10,000 rpm ($p = 0.08$) and achieved statistical significance at 12,000 rpm ($p < 0.05$). Interestingly, the subendocardial/subepicardial blood flow ratio in the LV wall, which was 1.17 ± 0.45 at baseline, remained relatively constant and unimpaired at all pump speeds (**Figure 8**). Regional blood flow in the kidneys (cortex, subcortex, and papilla) and brain (cortex, corpus medullare, cerebellum, and medulla spinalis) also did not change significantly from baseline levels as pump speeds increased (**Table 3**).

Discussion

In the present study, we observed that an increase in AoP_d associated with a slight increase in AoP_s and AoP_m led to a narrowing of pulse pressure with increasing pump speed. This effect, which was related to the increasingly predominant continuous flow characteristics associated with progressively reduced native cardiac pulsatility (LV unloading), was more pronounced at speeds above 10,000 rpm, which was consistent with previous experimental and clinical studies.[3] One

Table 2. Myocardial Blood Flow Measurements

	Pump Speed (rpm)			
	Pump Off (Baseline)	8,000	10,000	12,000
Septal wall				
Endocardium	0.46 ± 0.18	0.39 ± 0.20	0.30 ± 0.17	0.27 ± 0.16
Epicardium	0.38 ± 0.19	0.36 ± 0.20	0.34 ± 0.18	0.28 ± 0.15
Anterior wall				
Endocardium	0.48 ± 0.26	0.39 ± 0.20	0.30 ± 0.16	0.29 ± 0.21
Epicardium	0.38 ± 0.23	0.35 ± 0.23	0.25 ± 0.16	0.25 ± 0.15
Lateral wall				
Endocardium	0.43 ± 0.22	0.36 ± 0.20	0.29 ± 0.17	0.26 ± 0.15
Epicardium	0.39 ± 0.29	0.34 ± 0.19	0.28 ± 0.18	0.23 ± 0.20
Posterior wall				
Endocardium	0.36 ± 0.19	0.34 ± 0.17	0.23 ± 0.06	0.24 ± 0.11
Epicardium	0.37 ± 0.17	0.37 ± 0.21	0.27 ± 0.15	0.22 ± 0.15
Anterior wall + lateral wall + posterior wall				
Endocardium	0.42 ± 0.22	0.36 ± 0.18	0.27 ± 0.13*	0.26 ± 0.15**
Epicardium	0.38 ± 0.22	0.35 ± 0.20	0.26 ± 0.15	0.24 ± 0.16*

Values (ml/g/min) are mean ± SD.
* $p < 0.05$ *vs.* baseline.
** $p < 0.01$ *vs.* baseline.

Copyright © American Society of Artificial Internal Organs. Unauthorized reproduction of this article is prohibited.

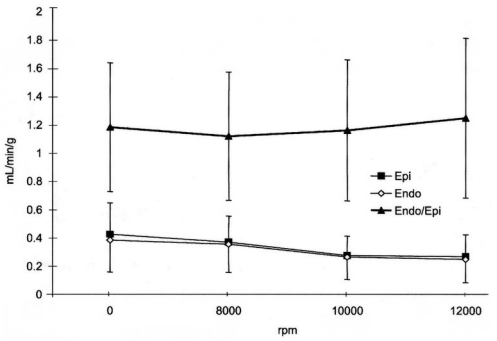


Figure 8. Tissue perfusion in subendocardium (Endo) and subepicardium (Epi) of left ventricular free wall.

cause of the increase in AoP_d was the reversal of blood flow direction, which occurred at speeds greater than 8,500 rpm (**Figure 5**); when combined with extensive LV unloading, this reversal contributed to the impairment of aortic valve opening at higher speeds (greater than 10,000 rpm). We also observed that the resulting reduction of systolic ejection caused blood to stagnate in the supravalvular regions, possibly leading to diminished myocardial perfusion *via* the epicardial arteries.

In our study, heparinization, prolonged exposure of intrathoracic tissue to air, and repeated blood sampling contributed to hypovolemia or anemia, which in turn became manifest in the symptoms of increased heart rate and decreased CVP, PAP, and hematocrit. To achieve hemodynamic stability at each increasing pump speed, CVP was maintained at 10–12 mm Hg, PAP at 20–25 mm Hg, HR at 75–90 bpm, and hematocrit above 30% by means of fluid or whole blood infusion. Hypovolemia was treated with crystalloid solution when the hematocrit was above 30% and with whole blood when the hematocrit was below 30%. We observed that the aortic valve stayed closed more frequently in hypovolemic calves, a problem that we found could be alleviated by fluid replacement at increasingly higher pump speeds. This observation is in concurrence with that of Westaby *et al.*,[12] who found that transfusion lessened the effects of left atrial collapse caused by extensive unloading of the left ventricle at high pump speeds. Thus achieving optimal LV filling and operating the pump at submaximal speeds appear to be essential to preserving normal aortic valve function and pulsatile blood flow. In addition, preserving normal aortic valve motion may produce the added benefit of washing out the aortic root and thus preventing thrombosis of the valve, coronary arteries, or both during pump support, as previously described by Frazier *et al.*[3] Several investigators have pointed out that partial unloading of the left ventricle may be more effective than total unloading,[13,14] which is recommended for achieving ventricular recovery[15] but can cause myocyte atrophy during long term support.[16,17]

Continuous removal of blood from the left ventricle with an LVAD (LV unloading) can decrease myocardial workload.[18] The gradual decrease in dP/dt at increasing pump assist rates may be attributed to delayed LV relaxation, which would be consistent with experimental findings by Saito et *al.*[19] In our study, the gradual decrease in CBF and MVO_2 at increasing pump speeds seemed to be related to effective unloading of the left ventricle and to reduced energy demand by the healthy myocardium secondary to decreased LV wall tension, as was previously shown in several studies.[20–24] Moreover, the CBF/MVO_2 ratio remained almost constant at increasing pump speeds, indicating that the decreases in CBF and MVO_2 were proportional to the decreased workload of the unloaded left ventricle and did not cause iatrogenic ischemia or impair LV wall function, as confirmed by intraoperative echocardiography. Similar findings by others support these observations. In a model of ischemia produced by LAD coronary artery ligation, Nakata *et al.*[25] showed that LVAD support restored LAD coronary artery flow by decreasing coronary vascular resistance secondary to reduced LVEDP. In experimental studies with an axial flow pump, Merhige *et al.*[5] and Smalling *et al.*[26] showed that coronary perfusion of the nonischemic myocardium decreased, while that of the ischemic myocardium increased after ventricular unloading. Consistent with the decrease we observed in CBF was the gradual reduction of regional blood flow to the left ventricle at increasing pump speeds, as detected by colored microsphere analysis. In addition, the constant endocardial/epicardial blood flow ratio in the LV free wall, even in reduced pulsatile aortic flow states achieved at pump speeds greater than 10,000 rpm, showed that the Jarvik 2000 pump did not adversely affect the autoregulation and transmyocardial distribution of CBF in the normal myocardium.

Little is known about the effects of nonpulsatile blood flow on cerebral microcirculation. Significant differences in intracerebral perfusion during both pulsatile and reduced pulsatile states in models of ischemia have been described.[6,27] We found that different regions of the central nervous system (and

Table 3. Tissue Perfusion Measurements

	Pump Speed (rpm)			
	Pump Off (Baseline)	8,000	10,000	12,000
Kidney				
Cortex	1.8 ± 0.7	1.5 ± 1.2	1.7 ± 1.4	1.6 ± 0.8
Subcortex	1.0 ± 0.6	0.8 ± 0.6	0.8 ± 0.8	0.9 ± 0.8
Papilla	0.8 ± 0.6	0.6 ± 0.4	0.6 ± 0.6	0.7 ± 0.6
Brain				
Cortex	0.4 ± 0.2	0.4 ± 0.3	0.4 ± 0.2	0.3 ± 0.1
Corpus medullare	0.2 ± 0.1	0.2 ± 0.2	0.2 ± 0.1	0.2 ± 0.1
Cerebellum	0.4 ± 0.3	0.4 ± 0.4	0.4 ± 0.3	0.3 ± 0.1
Medulla spinalis	0.3 ± 0.3	0.4 ± 0.4	0.3 ± 0.2	0.3 ± 0.1

Values (ml/g/min) are mean ± SD.

Copyright © American Society of Artificial Internal Organs. Unauthorized reproduction of this article is prohibited.

the kidney) were equally perfused at baseline (during a pulsatile state) and at higher pump speeds (during a diminished pulsatile state). Therefore, continuous flow did not appear to cause any microcirculatory shunting during end-organ perfusion in our study. This echoes the findings of Saito *et al.*,[4] who found no functional or histologic changes in major end organs during chronic support with a nonpulsatile LVAD.

The present study has some limitations. First, the Jarvik 2000 is designed to be used in patients with end-stage cardiac failure; therefore, our present results, obtained in a healthy animal model, may not be directly applicable to the clinical setting. This limitation might be addressed in the future by establishing an ischemic animal model in which the microcirculatory effects of the Jarvik 2000 on diseased myocardium could be assessed. Second, the present study relied on experiments performed in the acute setting when autoregulatory mechanisms were at work; consequently, the present findings do not necessarily warrant any conclusions about the long term effects of continuous flow on the myocardial microcirculation. Third, it was not possible to quantify or standardize the effects of the anesthesia performed and surgical trauma incurred during the pump implantation procedure, although the baseline hemodynamics of the study calves in the period immediately after pump implantation were normal. Finally, it is not clear what effect, if any, the choice of graft anastomosis site (*i.e.*, ascending *vs.* descending aorta) had on aortic and myocardial blood flow properties. Further studies in this regard are warranted.

In conclusion, our data suggest that the Jarvik 2000 pump may effectively unload the left ventricle and decrease MVO_2 secondary to reduced wall tension. Although the CBF decreases at increasing pump speeds as a result of reduced cardiac output, the CBF/MVO_2 ratio remains constant and does not impair normal LV function. Optimal adjustment of pump speed and LV volume allows the aortic valve to open and the native left ventricle to contribute to cardiac output even at maximum pump speed. Finally, microcirculation in the brain and kidney does not appear to be adversely affected at any pump speed.

References

1. Cooley DA: Initial clinical experience with the Jarvik 2000 implantable axial-flow left ventricular assist system. *Circulation* 105: 2808–2809, 2002.
2. Muller J, Wallukat G, Weng YG, *et al*: Weaning from mechanical cardiac support in patients with idiopathic dilated cardiomyopathy. *Circulation* 96: 542–549, 1997.
3. Frazier OH, Myers TJ, Gregoric ID, *et al*: Initial clinical experience with the Jarvik 2000 implantable axial-flow left ventricular assist system. *Circulation* 105: 2855–2860, 2002.
4. Saito S, Westaby S, Piggot D, *et al*: End-organ function during chronic nonpulsatile circulation. *Ann Thorac Surg* 74: 1080–1085, 2002.
5. Merhige M, Smalling R, Cassidy D, *et al*: Effect of the Hemopump left ventricular assist device on regional myocardial perfusion and function: reduction of ischemia during coronary occlusion. *Circulation* 80 (Suppl III): III158–III166, 1989.
6. Sezai A, Shiono M, Orime Y, *et al*: Major organ function under mechanical support: comparative studies of pulsatile and nonpulsatile circulation. *Artif Organs* 23: 280–285, 1999.
7. Macris MP, Parnis SM, Frazier OH, Fuqua JM, Jarvik RK: Development of an implantable ventricular assist system. *Ann Thorac Surg* 63: 367–370, 1997.
8. Henry WL, DeMaria A, Gramiak R, *et al*: Report of the American Society of Echocardiography Committee on Nomenclature and Standards in Two-dimensional Echocardiography. *Circulation* 62: 212–217, 1980.
9. Sidi A, Rush W: An alternative to radioactive microspheres for measuring regional myocardial blood flow, Part 1: colored microspheres. *J Cardiothorac Vasc Anesth* 10: 368–373, 1996.
10. Versieck J, Vanballenberghe L: Determination of tin in human blood serum by radiochemical neutron activation analysis. *Anal Chem* 63: 1143–1146, 1991.
11. Wester PO: Concentration of 24 trace elements in human heart tissue determined by neutron activation analysis. *Scand J Clin Lab Invest* 17: 357–370, 1965.
12. Westaby S, Katsumata T, Houel R, *et al*: Jarvik 2000 Heart: potential bridge to myocyte recovery. *Circulation* 98: 1568–1574, 1998.
13. Lisy O, Redfield MM, Jovanovic S, *et al:* Mechanical unloading versus neurohumoral stimulation on myocardial structure and endocrine function in vivo. *Circulation* 102: 338–343, 2000.
14. Maybaum S, Beniaminovitz A, Oz M, Di Tullio M, Savin S, Mancini D: Resting left ventricular size predicts improved native cardiac output during exercise and the ability to exercise with the device weaned in patients with the TCI HeartMate left ventricular assist device [abstract]. *J Heart Lung Transplant* 18: 44, 1999.
15. Goldstein D, Oz M, Rose E: Implantable left ventricle assist devices. *N Engl J Med* 339: 1522–1533, 1998.
16. Scheinin SA, Capek P, Radovancevic B, Duncan J, McAllister HA Jr., Frazier OH: The effect of prolonged left ventricular assist device support on myocardial histopathology in patients with end-stage cardiomyopathy. *ASAIO J* 38: M271–M274, 1992.
17. Kinoshita M, Takano H, Takaichi S, Taenaka Y, Nakatani T: Influence of prolonged ventricular assistance on myocardial histopathology in intact heart. *Ann Thorac Surg* 61: 640–645, 1996.
18. Goldstein AH, Pacella JJ, Clark RE: Predictable reduction in left ventricular stroke work and oxygen utilization with an implantable centrifugal pump. *Ann Thorac Surg* 58: 1018–1024, 1994.
19. Saito A, Shiono M, Orime Y, *et al*: Effects of left ventricular assist device on cardiac function: experimental study of relationship between pump flow and left ventricular diastolic function. *Artif Organs* 25: 728–732, 2001.
20. Frazier OH, Myers TJ: Left ventricular assist system as a bridge to myocardial recovery. *Ann Thorac Surg* 68: 734–741, 1999.
21. Maybaum S, Epstein S, Beniaminovitz A, Oz M, Bergman S, Mancini D: Resting myocardial blood flow and metabolism predicts improved native cardiac output and the ability to exercise with weaning in patients with the TCI HeartMate left ventricular assist device. *J Am Coll Cardiol* 33 (2 Suppl 1): 219A, 1999.
22. Beloni FL: The local control of coronary blood flow. *Cardiovasc Res* 13: 63–85, 1979.
23. Feigl EO, Neat GW, Huang AH: Interrelations between coronary artery pressure, myocardial metabolism and coronary blood flow. *J Mol Cell Cardiol* 22: 375–390, 1990.
24. Shiiya N, Zelinsky R, Deleuze PH, Loisance DY: Changes in hemodynamics and coronary blood flow during left ventricular assistance with the Hemopump. *Ann Thorac Surg* 53: 1074–1079, 1992.
25. Nakata K, Shiona M, Orime Y, *et al*: Effect of pulsatile and nonpulsatile assist on heart and kidney microcirculation with cardiogenic shock. *Artif Organs* 20: 681–684, 1996.
26. Smalling RW, Cassidy DB, Barrett R, Lachterman B, Felli P, Amirian J: Improved regional myocardial blood flow, left ventricular unloading, and infarct salvage using an axial-flow, transvalvular left ventricular assist device: a comparison with intra-aortic balloon counterpulsation and reperfusion alone in a canine infarction model. *Circulation* 85: 1152–1159, 1992.
27. Kono M, Orita H, Shimanuki T, Fukasawa M, Inui K, Wasio M: A clinical study of cerebral perfusion during pulsatile and nonpulsatile cardiopulmonary bypass. *Nippon Geka Gakkai Zasshi* 91: 1016–1022, 1990.

Copyright © American Society of Artificial Internal Organs. Unauthorized reproduction of this article is prohibited.